PHYSICAL REVIEW D

PARTICLES AND FIELDS

THIRD SERIES, VOLUME 37, NUMBER 4 15 FEBRUARY 1988

Probing the nature of the neutrino: The boron solar-neutrino experiment

R. S. Raghavan

AT&T Bell Laboratories, Murray Hill, New Jersey 07974

Sandip Pakvasa

Department of Physics and Astronomy, University of Hawaii at Manoa, Honolulu, Hawaii 96822

(Received 20 May 1987)

With a welter of neutrino scenarios and uncertain solar models to be unraveled, can solar-neutrino experiments really break new ground in neutrino physics? A new solar-neutrino detector BOREX, based on the nuclide ^{11}B, promises the tools for a definitive exploration of the nature of the neutrino and the structure of the Sun. Using double-mode detection by neutrino excitation of ^{11}B via the neutral-weak-current- and the charged-current-mediated inverse β decay in the same target, independent measurements of the total neutrino flux regardless of flavor and the survival of electron neutrinos in solar matter and a vacuum can be made. Standard models of the Sun, and almost every proposed nonstandard model of the neutrino, can be subjected to sharp and direct tests. The development of BOREX, based on B-loaded liquid-scintillation techniques, is currently in progress.

I. INTRODUCTION

The properties of the neutrino (ν) and their manifestations in weak-interaction phenomena play a central role in particle physics and its interfaces with astrophysics and cosmology. Of direct relevance to these fields are questions relating to nonvanishing ν masses, the structure of the mixing matrix of ν flavors, the stability of the ν, and the magnetic moment of the ν. Indeed, since the proton is not observed to decay, these questions define one of the few remaining test beds of grand unification and beyond.[1] It is increasingly apparent, however, that the answers are receding out of the range of experiments with laboratory ν sources such as accelerators, reactors, etc. An extraterrestrial ν source such as the Sun offers a long base line that could enhance sensitivity to nonstandard ν effects. The major impediment to this program is the evidence that the flux of solar ν's is seriously uncertain.

The unexpected low flux of solar ν's seen in Davis's ^{37}Cl ν experiment at Homestake,[2] as compared to the prediction of the standard solar model (SSM), points *either* to new properties of the ν *or* to new astrophysics of the Sun. Since the Homestake detector observes only electron neutrinos (ν_e), a flux loss by vacuum ν oscillations in transit, though *ad hoc* at best, cannot be ruled out. The alternate explanation seeks basic changes in the SSM, also largely *ad hoc,* conceding in effect that, as a ν source, the Sun is poorly defined. The dilemma hardly encourages the use of the Sun as a ν source for particle physics without incisive observational techniques that could separate the neutrino and astrophysics aspects of a solar-ν experiment.

Two recent developments, one theoretical and the other experimental, have changed the complexion of this field. It has been shown that the transport of ν's through the dense matter of the Sun allows resonantly amplified ν oscillations [the Mikheyev-Smirnov-Wolfenstein[3,4] (MSW) effect] with profound effects on the solar-ν spectrum and flux, even with very small flavor-mixing angles and mass parameters. The MSW effect unveils the Sun as a unique laboratory where subtle ν properties, generally inaccessible to terrestrial experiments, might be made observable.

On the experimental side, the "Rosetta stone" needed for interpreting solar-ν data may be within reach. ν's can be detected *regardless of their flavor* using ν excitation of nuclear levels (NUEX) via the neutral weak current by observing the sharp γ-ray line emitted by the deexciting nucleus.[5] The most promising target nucleus for NUEX is ^{11}B (Ref. 5). Flavor-sensitive ν_e spectroscopy is also possible in ^{11}B by charged-current- (CC-) mediated inverse β decay to a set of isospin-mirror levels in ^{11}C. These two features are tailored to the calibrative and investigative needs of the solar-ν problem. The NUEX mode is by nature insensitive to ν oscillations; it can thus *experimentally calibrate* the true solar-ν flux and "standardize" the Sun as a ν source. Relative to this calibrated ν output, the fluxes and spectra of the inverse β modes become specific measures of ν_e flavor survival under variables such as ν energy, path length, density of intervening matter, solar magnetic fields, etc. The NUEX standard thus lays the foundation for a penetrating study of the neutrino using the Sun as the source.

Expanding on our earlier note (Ref. 5) which dealt with principles of the NUEX experiment, in this paper we analyze as completely as possible the response of the ^{11}B detector to the various nonstandard models proposed for the neutrino and the Sun. We show that the NUEX and CC observables in the experiment respond with signatures that can distinguish practically every proposed nonstandard scenario. Based on a robust experimental route offered by standard liquid-scintillation techniques using industrially available B organic liquids, a moderate size detector containing some 100 tons of B ($\sim$600-ton total mass) should, in a year, lead to firm conclusions at least on the pressing questions such as ν oscillations and, thus, ν masses down to $\sim 10^{-4}$ eV. The flux of ^{8}B ν's, a sensitive thermometer of the solar core, can be directly measured subjecting the SSM to a critical test. We begin with a brief discussion of the technical and operational aspects of the ^{11}B detector now under development.

II. SOLAR-NEUTRINO DETECTION BY ^{11}B

Nuclear data.[5] Four basic reactions may be observed in the B experiment:

$$\text{(a) NUEX:}\quad \nu + {}^{11}\text{B} \to \nu' + {}^{11}\text{B}^*(E_i) \to \gamma(E_i) + {}^{11}\text{B}\ , \qquad (1)$$

$$\text{(b) CC:}\quad \nu_e + {}^{11}\text{B} \to e^- + {}^{11}\text{C}^*(E_i') \to \gamma(E_i') + {}^{11}\text{C}\ , \qquad (2)$$

$$\text{(c) } e-\nu\text{:}\quad \nu + e^- \to \nu + e^-\ , \qquad (3)$$

$$\text{(d) } \bar{\nu}_e p\text{:}\quad \bar{\nu}_e + p \to n + e^+\ ;$$

$$n + {}^{10}\text{B} \to {}^7\text{Li} + \alpha + 0.48\ \text{MeV}\gamma\ . \qquad (4)$$

Reactions (a) and (b) are specific to ^{11}B; (c) applies to all electrons and (d) applies to free protons in the detector. Figure 1 shows the level scheme of the ^{11}B-^{11}C isospin-mirror system. The ν-induced nuclear transitions are the NUEX mode to the doublet of levels at $\sim$5 MeV in ^{11}B and the inverse-β transitions (CC I–III) to the levels at energies E_i' in ^{11}C. The thresholds for NUEX events are just E_i, while those for the CC events are given by $E_{\text{th}} = E_i' + \Delta$, where Δ is the ^{11}B-^{11}C mass difference. In the CC transitions, electrons of energy $E_e = E_\nu - E_{\text{th}}$ are emitted; in the case of CC I and II, they are accompanied by the $\gamma(E_i)$. With a total event energy of $E = E_i' + E_e = E_\nu - \Delta$, these events reflect the incident ν_e *spectrum*. In contrast, NUEX events occur as sharp lines of energy $E = 4.5$ and 5 MeV, for $E_\nu > 4.5$ MeV, thus measuring the *total* ν *flux*. In practice, the ν events fall into two types: (1) "electron" events from a CC III ground state and from $e-\nu$ scattering and (2) "electron + γ" events from the excited-state transitions. The

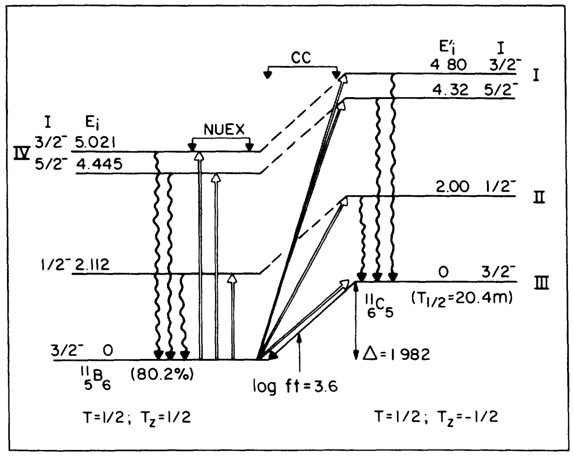

FIG. 1. The ^{11}B-^{11}C mirror nuclear system (E_i, E_i', Δ are in MeV).

NUEX and CC events are separable in practice as seen in the spectral profiles shown in Figs. 2(a) and 2(b). Background considerations indicate a practical low-signal bound at $E \approx 4$ MeV. The scintillation method also provides H atoms for reaction (d) which detects a $\bar{\nu}_e$ flux by a *delayed coincidence* of the prompt e^+ with the 0.48-MeV γ ray. The $\bar{\nu}_e$ energy (≥ 4 MeV) can be derived from the e^+ energy.

In standard electroweak theory, the excitation strength for NUEX, λ_{NX}, is directly related to the

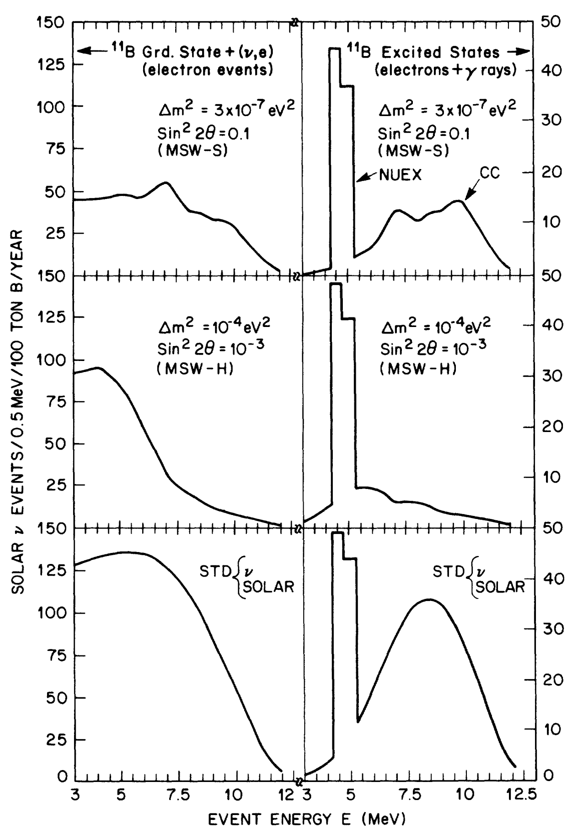

FIG. 2. (a) Left panels, (b) right panels. Spectral profiles of solar-neutrino events in the B experiment [ν fluxes from SSM(B)]. The ν energy E_ν=event energy E + 1.982 MeV.

Gamow-Teller strength B (GT) of the mirror CC transition. For the ^{11}B-^{11}C system:[5,6]

$$4\lambda_{NX}=\lambda_{CC}(\text{mirror})=G_A^2 B(\text{GT})\ (\text{mirror})\ , \quad (5)$$

where $G_A=1.26$ is the axial-vector–vector coupling ratio. Preliminary B(GT) data for ^{11}B are now available from (p,n) reaction work[7] standardized directly by the B(GT) for the ground-state transition (CC III) given by the ft value of the ^{11}C decay. The λ_{NX} can also be derived from radiative data using the relation[5]

$$\lambda_{NX}=0.2963\kappa B_{ISV}(M1)\uparrow\ , \quad (6)$$

where $B_{ISV}(M1)\uparrow$ is the isovector dipole ($M1$) spin-excitation strength derived from (γ,γ) or (e,e') data and $\kappa\approx 0.75$ allows for "quenching" of the weak relative to the γ strength. They are in good agreement with those from Eq. (5) (Ref. 8). The ν cross sections for the B experiment are thus firmly in hand. Solar-ν yield rates can thus be obtained using the phase-space factors appropriate for NUEX and CC transitions.[5] (See the Appendix for details of these calculations.) The $(e-\nu)$ event yields can be computed using standard theory.[9]

Detector techniques. The ^{11}B experiment can be performed by B-loaded liquid-scintillation (LS) spectroscopy,[10] a simple, versatile, time-tested, low-energy technique. Efficient LS systems using trimethyl-borate [TMB:$B(OCH_3)_3$] mixtures ($\sim 7\%$ B) are routinely used for slow-neutron detection.[10] A new B-rich LS system ($\sim 15\%$ B) with trimethoxyboroxine [TMBX:$B_3O_3(OCH_3)_3$], a TMB derivative with very similar properties, appears so far to be the best choice. Both the liquids are extremely transparent and thus ideal for large-scale LS detectors. Good quality solar-ν spectra can thus be expected from this approach. An important practical convenience is that the B liquids are industrially available at reasonable cost.

The principal experimental challenge lies in achievement of *low-energy* (few MeV) spectroscopic capability in a *large-scale* detector which is more typical of high-energy physics. In this respect the experience of Kamiokande II (K II) provides great encouragement.[11] A 2000-ton pool of water placed underground was observed by 1000 phototubes, recording the energy and location of nuclear events down to ~ 7 MeV by Cherenkov spectroscopy. The threshold is set mainly by the poor Cherenkov light yields at lower energies. Thus a logical extension of this experience to lower energies is to apply the same techniques to a massive detector containing boron-loaded scintillation liquid instead of water. The ~ 40-times more light available in this method should enable much lower energy thresholds and spectroscopy with much higher energy, time, and spatial resolutions than was possible at K II. The current development of the boron experiment is thus based on the concept of a large tank of boron-loaded LS observed by a large number of photodetectors. While the attainment of low thresholds is possible, the viability of this concept then depends crucially on limiting the high backgrounds typical at these energies. Great care is thus necessary in the design of the detector and we sketch some of the principal considerations.

Sources and control of background. The background in the ^{11}B experiment arises from sources external and internal to the detector and depends strongly on the energy. Cosmic-ray muons create nuclear excitation and radioactivity by primary and secondary reactions. While prompt activities with short lifetimes can be vetoed by the large muon signal, long-lived ($\sim$sec) activities create large veto dead times if the muon rate is high. The spatial resolution available in the detector is helpful since the muon tracks can be localized tightly, keeping the average dead fraction of the detector within tolerable limits. The advantage is important since relatively shallow mines [typical of the Irvine-Michigan-Brookhaven (IMB) or Kamioka nucleon decay (Kamiokande) detectors] come into consideration as viable sites for the ^{11}B experiment.

These large underground pools of water are, in fact, nearly ideal since they provide the advantage of a thick water shield, necessary to cut down (by several orders of magnitude) the low-energy background "glow" and its pile-up tail at high energies, as well as reduce the real high-energy (n capture and fission) γ rays from the rock ambience of the mine. B doping the water ($\sim 0.1\%$) suppresses neutrons without generating high-energy capture γ rays because of its high (n,α) cross section (800 b). B in the detector itself self-shields against internal n-capture γ rays from structural material.

The major unshielded source is U/Th activity in the active scintillator volume itself. The focus is thus on the *radiopurity of the B liquid* and on the background in the region $3<E<6$ MeV in the window of the NUEX signal, which has the lowest yield rate and event energies. The radioactivity of ^{238}U and ^{228}Th in equilibrium with their daughters produces α's up to 9 MeV in energy, β rays up to 3.2 MeV, and γ rays up to 2.6 MeV. The 2.6-MeV γ ray occurs in coincidence with β and γ cascades summing to a total energy up to 5 MeV, thus tailing into the NUEX window. Assuming some suppression of such events by their spatial patterns, we estimate that a radiopurity of ~ 0.01 parts per trillion (ppt) of U/Th of the LS material is necessary to restrain this background below the NUEX signal levels ($S/N\sim 1$). The investigation of radioactivity in the B materials of interest and development of methods to control them in the industrial production processes form the major part of the development work.

The α emission of U/Th also creates γ rays in the NUEX window by reactions on B itself: $^{11}B(\alpha,n\gamma)\,^{14}N^*$ (3.95, 4.91, 5.1 MeV) with thresholds at -5.5 and -6.5 MeV and $^{10}B(\alpha,p\gamma)\,^{13}C^*$ (3.68, 3.85 MeV) with $Q=\sim 0$. C, O, and H in a typical LS mixture are inert to α's because of high Q values. The high thresholds of ^{11}B $(\alpha,n\gamma)$ are helpful since only the highest-energy α's such as those from ^{214,212}Po decays are then potent; even these follow energetic β, γ precursors after a time delay and thus can be identified. α-induced γ rays are thus mainly due to lower-energy α reactions on the 20% ^{10}B content of the target. Although some neutrons from B(α,n) can produce the very γ rays of a NUEX signal by $^{11}B(n,n'\gamma)$ ($E_n>5$ MeV), these events are much rarer. For the limit of U/Th at 0.01 ppt set already, α-induced γ rays are estimated to be only $\sim 1\%$ of the β-γ cascade background.

The spectral profile of background is distinct from the NUEX signature; i.e., it appears as a continuum under the sharply defined NUEX lines. Because of this profile, a design criterion of $S/N \sim 1$ may be adequate to assure reliable observation of the NUEX events. At this level the S/N for the stronger, higher-energy CC signal is expected to be at least an order of magnitude higher.

Background from antineutrinos. The CC/NUEX ratio, a key experimental objective, becomes uncertain if a flux of $\bar{\nu}_e$'s with sufficient energy is present, since they contribute to NUEX but not CC event yields. Possible sources of $\bar{\nu}_e$'s are primordial radioactivity in Earth (too low energies to interfere), prevalence of nuclear power reactors, and relic $\bar{\nu}$'s from past supernova events. The highest $\bar{\nu}_e$ flux, that is due to reactors, is estimated at Gran Sasso[12] to be about $4.5\times 10^5/\text{cm}^2\text{sec}$ (5% of the solar flux). From known reactor $\bar{\nu}_e$ spectra, we calculate that they can add $\ll 1\%$ to the NUEX signal. Estimates of the supernova relic $\bar{\nu}$ flux,[13] although uncertain, indicate a negligible contribution. In the LS method, a $\bar{\nu}_e$ background can be experimentally detected by reaction (d) since protons are available in the organic B liquids.

III. OBSERVABLES IN NONSTANDARD SCENARIOS

The Homestake experiment indicates the need for revising the standard model of at least one of the two basic ingredients of solar-ν science: viz., the structure of the Sun and the nature of the ν. Experiment must decide which, and as far as possible, how. In the ^{11}B experiment, the tools available for this program are (1) the NUEX signal, (2) the CC signal and the CC to NUEX ratio, (3) the CC spectral shapes, and (4) time variations of the signals. We now briefly survey (Table I) the responses of these observables to nonstandard scenarios.

Nonstandard solar models. It is generally agreed that although most of the signal in the ^{37}Cl Homestake experiment must arise from high-energy ^{8}B ν's, low-energy

TABLE I. Response of ^{11}B solar-ν experiment to nonstandard scenarios. (Yields from ^{37}Cl and ^{71}Ga are also shown for comparison.) (Δm^2 values in eV^2.) Definitions: N/N_0: NUEX signal (N_0 referred to 5.9 SNU-SSM for correspondence only); S = fractional CC signal survival *relative to ν flux determined by N*; A = (high/low) spectral asymmetry; D = night/day signal ratio; $S_M = S$ *relative to ν flux of 5.9 SNU-SSM only.*

Scenario	^{11}B N/N_0	S	A	D	^{37}Cl S_M	^{71}Ga S_M
New solar model	<0.3	1	1	1	0.25–0.45	~0.85
Vacuum ν osc.[a]						
($\sin^2 2\theta \approx 1$)						
($\Delta m^2 > 10^{-9}$)	1	0.33	1	1	0.33	0.33
MSW-H						
($\sin^2 2\theta \sim 5\times 10^{-4}$–0.2)						
($\Delta m^2 \sim 10^{-4}$)	1	0–0.4	0–0.5	1	0.25–0.45	~0.85
MSW-S						
($\sin^2 2\theta \sim 5$–40×10^{-4})						
($\Delta m^2 \sim 1$–7×10^{-5})	1	0–0.26	2–4	1	0.25–0.45	~0.85
($\sin^2 2\theta \sim 4$–300×10^{-3})						
($\Delta m^2 \sim 1$–100×10^{-7})	1	0.35–0.55	1.25–1.6	1	0.25–0.45	0–0.5
MSW-V						
($\sin^2 2\theta > 0.3$)	1	0.25–0.45[b]	1		0.25–0.45[b]	0.25–0.45[b]
($\Delta m^2 \sim 1$–10×10^{-6})		0.1–0.33[c]		1.25–4	($D<3$)	($D\sim 1$)
($\Delta m^2 \sim 0.5$–10×10^{-7})				~1	($D\sim 1$)	($D<3$)
Nonflavor ν osc.						
$\nu_{eL}\to\eta_{eL}$; Vacuum[d]	0.5	1	1	1	0.5	0.5
$\nu_{eL}\to\eta_{eL}$; Matter	0–0.58	1	Same as in MSW			
ν moment		Semiannual and 11 yr solar-cycle anticorrelation				
$\nu_{eL}\to\nu_{eR}$	<1 (var.)	1	1	1	<1	<1
$\nu_{eL}\to\nu_\mu^c, \nu_\tau^c$	1 (inv.)	<1	1	1	<1	<1

(a) Three-flavor mixing.
(b) Day-night average.
(c) Day yield.
(d) Two-state mixing.

ν sources in the Sun also contribute to the extent of $\sim 25\%$. Since the observed signal itself is a fraction of this order,[2] the focus of solar-model revisions is to engineer a strong suppression of the flux of ^{8}B ν's along with a moderate reduction of the lower-energy ν flux from the decay of ^{7}B (Ref. 14). The ^{11}B experiment is sensitive *only* to ^{8}B ν's. This experiment is thus more sensitive to solar models than ^{37}Cl. In the two "standard" models, SSM(A) [5.9 SNU (solar-neutrino unit) for ^{37}Cl] (Ref. 15) and SSM(B) (Ref. 16) (8 SNU) of Bahcall *et al.*, the ^{8}B flux differs by $\sim 50\%$. Other models, e.g., that of Faulkner and Gililand (C),[17] predict 9.25 SNU. To reach the 2σ upper limit of 2.7 SNU of the ^{37}Cl signal, nonstandard models need to reduce the ^{8}B flux by a factor of ~ 2.5 to ~ 4.5 depending on the standard framework. It may be mentioned that many of the genuine attempts at solar-model revisions are in conflict with observations of solar seismic oscillations.[18] A new idea based on the presence of weakly interacting massive particles (WIMP's) in the Sun,[17] predicts ^{37}Cl signals down to 1 SNU with assumptions on the abundance and mass of the WIMP's. It is the only *nonstandard* model [along with SSM(A)–(C)] that agrees well with seismic oscillation data.[18] Since WIMP's are generally thought to be relevant for the other outstanding astrophysical puzzle, viz., the dark-matter problem, this model has received recent attention.[1] We conclude that the NUEX signal (and equally the CC) in ^{11}B would be reduced at least by a factor of 4, typically more severely than the ^{37}Cl signal. The main thrust of solar-model revision would thus be confirmed by a markedly poor signal in the ^{11}B experiment. By the same token, a reasonable NUEX signal can uniquely determine the ^{8}B flux, a result obviously of fundamental astrophysical interest.

Nonstandard neutrinos. New solar models, though varied in astrophysical detail, all produce the same effect on the ^{11}B experiment, viz., a serious loss of signal. In contrast, the different nonstandard models of ν's promise a rich variety of effects with sizable signals involving several observables. The ν phenomena most widely considered are ν oscillations in a vacuum[19,20] and in matter (the MSW effect),[3,4] and the effect of a finite-ν magnetic moment.[21]

Indicator of new neutrino physics. Equation (5) constrains the NUEX and its isospin mirror CC (I) signals to a fixed ratio independent of the details of nuclear structure of the states involved. Since the strengths of all the CC and the (e,ν) reactions are known relative to CC (I), the signal ratio [total CC + (e,ν)]/NUEX is also a fixed number S_0. An experimental signal ratio S' will have the value of S_0 if and only if the detected ν flux consists *wholly* of ν_e's. Defining a CC signal "survival" fraction S as $S = S'/S_0$, observation of $S<1$ would be compelling evidence for *nonconservation of* ν_e *flavor.*

Neutrino flavor oscillations in a vacuum. Neutrino oscillations are important in particle physics because they offer a direct way to search for the existence of a ν mass spectrum and a possible nonconservation of lepton flavor, both primary requirements for the effect. Solar ν's at present are especially exciting as they promise a unique window on ν masses as small as 10^{-4} eV or smaller and indirectly on mass scales as large as 10^{15} GeV.

When ν's have nonzero masses, in general, the weak eigenstates ν_x $(x = e,\mu,\tau)$ are related to the mass eigenstates ν_i (masses m_i) by a mixing matrix. If a specific flavor, say ν_e, is produced at time $t=0$, the differing phase changes produce a time-dependent mixture of flavors. The survival of the ν_e flavor at a distance L depends on the mixing angles θ_{ij} and the mass differences $\Delta m_{ij}^2 = m_i^2 - m_j^2$ which occur in the oscillatory part in the form $\Delta m_{ij}^2/E_\nu$. For $\Delta m_{ij}^2 \geq 10^{-9}$ eV^2 and *maximal* mixing, the ν_e (and the CC) survival fraction is $S=\frac{1}{3}$ for three flavors.[22] The suppressions of CC yields are identical for all solar-ν detectors and the CC spectral shapes are undistorted. Only for $\Delta m_{ij}^2 \ll 10^{-10}$ eV^2 (and for maximal mixing) can $S<\frac{1}{3}$ occur, albeit with considerable fine-tuning of Δ_{ij}^2 (Ref. 22). The ν_e flavor loss is energy dependent in this mass range; thus, spectral distortion and variation of yield with detectors can be expected. The general prejudice against vacuum oscillations is that they affect solar ν's *only* for the special case of maximal flavor mixing.

The MSW effect. Wolfenstein first showed[4] that for ν transport through matter the above description is incomplete since it omits the interaction of ν's with electrons. ν_e's scatter on electrons via the neutral currents as well as CC, while ν_μ and ν_τ scatter only via neutral currents. Thus ν_e's move in a potential which depends on the density of electrons in the medium, altering the ν_e propagation phases. The importance of this effect for ν_e's traversing dense solar matter was first realized by Mikheyev and Smirnov[3] who showed that the potentials present in the Sun can compensate the vacuum phase $(\Delta m^2/2E_\nu)$ and, in effect, "amplify" even a small intrinsic mixing angle to the maximum value and fully convert a ν_e to ν_μ or ν_τ. The dependence of the MSW resonance on E_ν can produce striking changes in the observed *CC signal yields* and *spectral shapes* for $\Delta m^2 \leq 10^{-4}$ eV^2 for the entire range of $\sin^2 2\theta > 5\times 10^{-4}$.

Several authors have solved the MSW equations for the solar regimes.[23–26] The results for the ^{11}B ground-state CC III transition are displayed in Fig. 3 as contours of constant CC survival fraction S on a map of Δm^2 vs $\sin^2 2\theta$. The CC yield decreases toward the interior of the "MSW triangle." The shaded band is the parameter space compatible with a 2σ-range of the ^{37}Cl result (1.5 to 2.7 SNU) relative to SSM(A) (5.9 SNU). [The range of SSM(B) (7.5 SNU), though mostly covered, extends more inward, allowing smaller S values.] The MSW effect implies a CC survival S of 0 to 55% for the ^{11}B experiment.

The result of the effect is different on the three sides of the MSW triangle. The smallest S factors occur in the horizontal band (MSW-H: $\Delta m^2 \approx 10^{-4}$ eV^2). Here, ν_e's of $E_\nu > 2$ MeV, in the entire range of CC sensitivity, can be resonantly converted as the cutoff energy decreases to the lower bound. The energy dependence also distorts the CC spectrum as shown by Fig. 2 (middle). It is markedly asymmetric compared to the standard profile (Fig. 2, bottom) since the cutoff, here at $E_\nu \approx 9$ MeV,

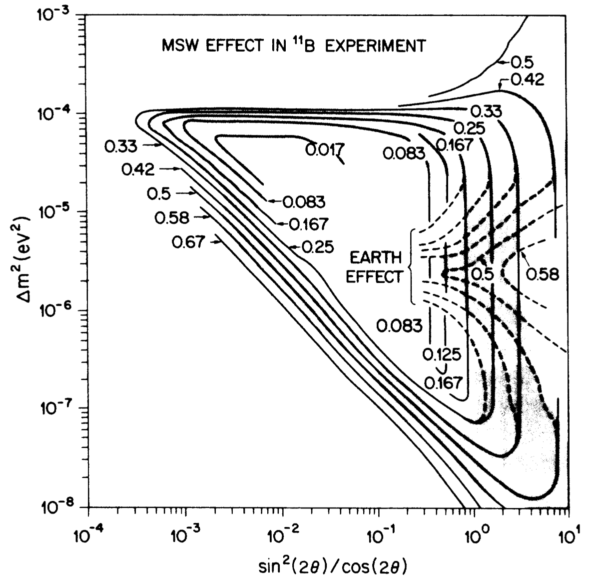

FIG. 3. CC survival fraction S for ν parameters Δm^2 and ($\sin^2 2\theta/\cos 2\theta$) relevant to the MSW effect. The solid lines are iso-S contours. The shaded region is the space compatible with the Homestake experiment according to 5.9 SNU SSM(A) (reproduced with kind permission from A. J. Baltz).

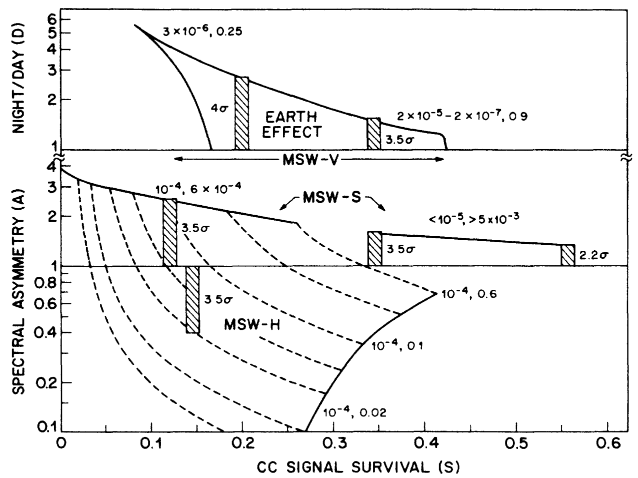

FIG. 4. Experimental observables of the MSW effect (in the parameter space compatible with the Homestake experiment). The asymmetry A is defined as the spectral ratio "high" ($E > 7.5$ MeV)/"low" ($E = 4-7.5$ MeV). The solid lines in both upper and lower panels for $S < 0.4$ are limiting values of A and D. For $S > 0.35$, in MSW-S, they are the only observable values. Dashed lines are for constant high fraction (given by the S value at the intercept with the $A = 1$ line). The pairs of numbers indicate representative values of Δm^2, $\sin^2 2\theta$ which apply to the effect observed. The vertical bars are estimates of precision with which the "effect" can be distinguished from a "no effect" ($A,D = 1$), in a BOREX design of ~ 100 tons of B.

suppresses high-energy ν_e's. Along the sloped side of the triangle (MSW-S), the cutoff energies are *less than* 6 MeV. Thus, in this regime, only the lower energy ν_e's are converted, producing *reversed* asymmetries in the CC spectra. Figure 2 (top) demonstrates the shift of spectral weightage toward higher energies. Furthermore, the highest ^{11}B CC yields are to be found in the MSW-S regime. The effect along the vertical side (MSW-V: moderately large mixing angles) is independent of Δm^2. The CC survival is given by $\sin^2\theta$ regardless of energy. Thus, in MSW-V, the average CC signal loss in ^{11}B is the same as in ^{37}Cl and the spectra are undistorted.

Earth effect and day-night variation. Solar ν_e's converted to ν_μ's by the MSW effect in the Sun can be regenerated by passage through Earth, thus increasing the nighttime flux of ν_e's and the signal intensity.[26–28] The dashed lines in Fig. 3 indicate how the Earth effect changes the MSW contours at night (for a typical northern latitude at equinox). The effect is significant for $10^{-5} < \Delta m^2 < 10^{-6}$ eV^2 in the MSW-V region, i.e., for "large" mixing angles. The actual differences depend on the season, winter effects being larger than in summer. A confirming signature is the constancy of the NUEX signal.

The three observables useful for identifying the MSW effect and deriving ν parameters are the CC signal survival S, the asymmetry A defined as the ratio of the high- and low-energy CC spectral yields (normalized to the standard CC spectral shape), and the night/day ratio D. The S-A and S-D correlations predicted by the MSW effect are summarized in the plot of Fig. 4. The limiting lines reflect the allowed band of Fig. 3 [SSM(A)]. SSM(B) implies limits at smaller S values; however, since A and D then tend to increase, experimental sensitivity is maintained. Thus, in general, the effect of the three MSW regions are, to a large extent, uniquely identifiable in the experiment.

Neutrino oscillations into sterile states. Speculations have been made on the occurrence of ν oscillations not between ν flavors but between ν_{eL} and a hypothetical neutral particle η_{eL} which is a singlet under SU(2)$\times$U(1) and is "sterile" in all weak interactions.[29,30] If they exist at all, nonflavor oscillations can be uniquely identified in the B experiment. The phenomenology is similar to flavor oscillations (vacuum and MSW) and thus the effects on the CC signal such as spectral asymmetry and the night/day variation are the same. The effect on the NUEX signal, however, is different. Unlike converted ν_μ or ν_τ, which can be observed by NUEX, η_{eL} is sterile and cannot be detected at all. Thus the NUEX signal is *reduced* by the same factor as the CC signal, resulting in $S = 1$, as distinct from $S < 1$ for flavor oscillations. Sterile oscillations in some MSW-V regions ($A = 1$; $D \sim 1$) thus create only a gross signal loss similar to a solar-model effect; but they also create the *same* loss in the ^{37}Cl and the Ga (Ref. 31) experiments. In contrast, proposed solar models affect the three experiments *unequally* since they are each sensitive to different ν sources in the Sun.

Neutrino magnetic moment. Recently, several authors claimed to have observed an *anti*correlation of the Homestake ^{37}Ar yield with the 11-yr solar activity cycle.[2] It has revived an old explanation[32] based on the interaction of a possible ν magnetic moment with solar magnetic fields to explain the correlation to solar activity and also predict a semiannual variation of the effect.[21] If the ν moment is $\sim 10^{-10}\mu_B$, the intensity and spatial extent of known solar magnetic fields[21] can convert left-handed ν_{eL}'s into right-handed ν_{eR}'s which elude CC weak processes and escape detection at Homestake. Theoretically, a plausible model to explain such a large-ν magnetic moment appears difficult. In the B experiment, a similar loss of the CC signal correlated with solar activity and a possible semiannual variation should be observed; no specific spectral effects are expected. However, the effect on NUEX depends on the nature of ν_{eR}. If ν_{eR}, the Dirac partner of ν_{eL}, is a new sterile particle[21] the NUEX signal would also vary exactly as the CC ($S=1$). But if it is identified with the charge conjugates ν_μ^c or ν_τ^c (Ref. 21), then the NUEX signal is unaffected.

The above discussion covers almost every nonstandard model advanced for the neutrino and the Sun. Their effects on the observables of the B experiment, summarized in Table I, are distinct enough so that, barring pathologically combined scenarios, each of these models can be distinguished clearly. The discrimination afforded by the NUEX standard largely underlies this capability.

IV. CONCLUSIONS AND OUTLOOK FOR BOREX

The basic specification which determines the overall magnitude of resources and effort in the B solar-ν experiment BOREX is the mass of the boron target. It is determined by the signal rates and the sizes of the effects required in the experiment to achieve its scientific aims. The firm nuclear cross sections and the response of BOREX to nonstandard scenarios summarized in Fig. 4, provide the framework for this optimization.

The primary scientific aim of BOREX is to establish with at least 90% confidence whether or not ν oscillations exist and, if so, to derive the ν parameters as uniquely as possible. In practice, this entails a demonstration of *either* (1) a specific ν effect, such as spectral asymmetry or time variation (daily, half-yearly, or 11 yr), i.e., A, D, etc., $\neq 1$ at the 2σ level, *or* (2) that the CC survival fraction S deviates (or not) by 2σ from unity.

Taking the putative case of *either* a solar-model effect *or* ν oscillations as the prevailing scenario, the practical conditions for meeting the above requirement can be inferred from Fig. 4. It shows typical precisions that can be achieved in the measurement of A and D for various regions of the MSW map for a BOREX design with 100 tons of B, operating for 1 yr. The estimates are based on the smallest predicted ^{8}B ν flux of SSM(A), an electron detection efficiency of 100%, and a reasonable CC background through $E=4-12$ MeV extrapolated from a level of $S/N=1$ for the NUEX signal. It is seen that for almost all the ν parameter space covered by the MSW map, at least requirement (1), and generally both (1) and (2) above, can be satisfied. In addition, ν moment effects can produce time variations anywhere in and outside the MSW parameter space. If such effects are small, then the remaining ν scenario, that of vacuum oscillations which appear spectrally identical to the effect of solar-model revision, can still be exposed by appealing to the S value which is $\frac{1}{3}$ vs 1 for the two cases. The experimental precision of S depends mainly on that of the NUEX yield, which can be determined to an accuracy of $\sim 30\%$ in BOREX under the same assumptions as above. This assures that the two scenarios can be distinguished. As we go to higher fluxes from model (A) to (C), the precision becomes better, $\sim 20\%$. We conclude that with no apparent exceptions, ν oscillations can be identified and thus our experimental aims adequately met with in this minimal BOREX design.

If ν oscillations do occur, then Fig. 4 and Table I show that the various ν scenarios proposed so far can be uniquely distinguished from each other. ν mass differences and mixing angles can be inferred from the identification of the particular MSW action observed. We conclude that this BOREX design will enable a definitive experimental study of the nature of the neutrino.

The minimal BOREX design (~ 100 tons of B) implies a solar-ν detector of overall mass of ~ 600 tons. It thus compares well with other solar-ν proposals such as Sudbury Neutrino Observatory,[33] a 1000-ton heavy-water detector and ICARUS,[34] a 3600-ton liquid Ar chamber. The experimental development of BOREX is being carried out at AT&T Bell Labs and elsewhere.

ACKNOWLEDGMENTS

We have benefited from discussions and generous help from several colleagues, in particular, J. Bahcall, A. J. Baltz, B. A. Brown, W. L. Brown, E. Chandross, M. Deutsch, X-G. He, J. Learned, J. W. Mitchell, S. P. Rosen, R. Steinberg, and J. Weneser, all of whom we thank sincerely. The work of S.P. was supported in part by a grant (DE-AN03-76SS00235) from the U.S. Department of Energy.

APPENDIX: CC AND NUEX EXCITATION STRENGTHS IN A ^{11}B-^{11}C SYSTEM

1. Event rates

The solar-ν event rates for NUEX and CC modes in the Boron experiment are as follows.

(a) NUEX transitions:

$$Y_{NX}=\frac{G_F^2}{\pi}\phi\lambda_{NX}P_{NX}\ ,$$
$$Y_{NX}=1.68\times 10^{-44}\phi\lambda_{NX}P_{NX}/^{11}\text{B nucleus/sec}\ , \qquad (A1)$$

where ϕ = solar-ν flux $=6.0\times 10^6$/cm^{2}sec; λ_{NX} = NUEX strength $=\frac{1}{4}G_A^2\langle\sigma\tau_z\rangle^2$; $G_A=1.26$; P_{NX} = phase-space factor $=\int S(E_\nu)(E_\nu-E_{th})^2dE_\nu$ with $S(E_\nu)$, the incident ν spectral profile; energies are in MeV.

(b) Charged-current (inverse-β) transitions:

$$Y_{CC}=1.68\times 10^{-44}\phi\lambda_{CC}P_{CC}\ , \qquad (A2)$$

where λ_{CC} = CC strength $=G_A^2\langle\sigma\tau_-\rangle^2=G_A^2B(GT)$; $P_{CC}=\int S(E_\nu)W_ep_eF(Z,W_e)dE_\nu$; with $W_e=(E_\nu-E_{th}+0.511)$; $p_e=(W_e^2-0.511^2)^{1/2}$; and $F(Z,W_e)$ is the Fermi function (≈ 1.14 for $Z=6$).

TABLE II. CC strengths for ^{11}B-^{11}C transitions.

State in ^{11}C	$B(\text{GT})_{\text{expt}}$	λ_{CC}
0	0.345(8)	0.548 + 1.0
2.0	0.40(4)	0.635
4.32 + 4.8	0.955(90)	1.52

2. Relation between λ_{NX} and λ_{CC}

The boron system is an isodoublet mirror pair ($T=\frac{1}{2}$). Within this doublet, the operators of the transitions from the ^{11}B ground state to an excited state (NUEX) and the inverse-β reaction to the corresponding excited mirror level in ^{11}C are related as

$$\langle \sigma\tau_z \rangle^2 = \langle \sigma\tau_- \rangle^2 \quad (T=\tfrac{1}{2}) .$$

Thus from the definitions of λ_{NX} and λ_{CC} the following relation holds:

$$4\lambda_{\text{NX}} = \lambda_{\text{CC}} = G_A^2 B_{\text{GT}} . \tag{A3}$$

3. How to get λ_{CC} and λ_{NX}

(a) Charged-current λ_{CC}: For the ground-state transition ^{11}B-^{11}C, the ft value is known: $\log ft = 3.6$. Thus, λ_{CC} is given by

$$\lambda_{\text{CC}} = B(F) + G_A^2 B(\text{GT}) = 6165/4000 = 1.55 , \tag{A4}$$

where 6165 sec is ft for $\lambda_{\text{CC}}=1$ (superallowed 0-0 decay), $B(F)$ is the Fermi and B(GT) the Gamow-Teller matrix elements. For this ground-state mirror pair, $B(F)=2T=1$. Therefore, $B(\text{GT})=0.345(8)$ (Ref. 35). For the excited states, $B(F)=0$. [For the 2.0- and 4.3-MeV levels in ^{11}C, $B(F)=0$; for the 4.8-MeV level, $B(F)\approx 0$ within 5%.] Thus they proceed only by B(GT). The B(GT) values have been determined by Taddeucci *et al.*[7] at the Indiana cyclotron using (p,n) reactions on ^{11}B at 0° with 160- and 200-MeV protons. Two kinds of measurements were made: (1) differential cross-section measurements and (2) a spin transfer by polarization measurement. These two parameters were measured for the ground and excited states in ^{11}C. They are proportional to B(GT). Since the B(GT) for the ground-state transition is known (see above), the self-calibration allows absolute B(GT) of the CC transitions to the excited states to be evaluated from these results. The differential cross-section and polarization measurements agree within 10% which is the order of the uncertainty of these determinations. The results are given in Table II.

It is worth stressing that for ^{11}B the B(GT) values are based on *relative* measurements in the same target and the states of interest are well resolved from each other and from the ground state. The uncertainties inherent in B(GT) values from (p,n) reaction are important mainly for cases where *no internal calibration is available.* This does not apply here.

(b) Neutral current λ_{NX}. Since λ_{CC} is known, relation (A3) can be directly used to get λ_{NX} for the excited states, in particular to the (4.45 + 5.0) MeV doublet in ^{11}B.

4. Derivation of λ_{NX} from radiative data

The λ_{NX} for the excited states in ^{11}B can also be obtained from the *measured radiative widths* of these levels. For our earlier paper[5] the (p,n) results were not yet available and we calculated λ_{NX} by this method and obtained λ_{CC} using Eq. (A3). Now these calculations serve as a check of the applicability of Eq. (A3) for mirror pairs and also as a reverse consistency check of the (p,n) results. The radiative widths for ^{11}B have been measured[36] by (e,e') scattering or resonance fluorescence (γ,γ'). These measurements yield the widths Γ_0 and thus the reduced $M1$ strength $B(M1)$ for decay to the ground state. The excitation strength $B(M1)\uparrow$ is then known by using the spin statistical factors. It can be shown that[5]

$$\lambda_{\text{NX}} = \tfrac{1}{4} G_A^2 \langle \sigma\tau_z \rangle^2 = G_A^2 \frac{4\pi}{3} \frac{1}{(\mu_n - \mu_p)^2} B_{\text{ISV}} M1\uparrow , \tag{A5}$$

where $B_{\text{ISV}}M1\uparrow$ is the isovector $M1$ spin excitation strength. We derived $B_{\text{ISV}}M1\uparrow$ from the measured $B(M1)\uparrow$ as follows. A theoretical calculation of the $B(M1)\uparrow$ values of the excited states was made with a shell-model code which gave values in reasonable agreement with the measured $B(M1)\uparrow$. Then the isovector spin part of the $M1$ strength was calculated with the same wave functions. The ratio of the two theoretical values provided a factor for each excited state. This factor was applied to the *measured* $B(M1)\uparrow$'s and taken as the values for $B_{\text{ISV}}M1\uparrow$. Next, this was used in Eq. (A5) to derive an "uncorrected" λ_{NX}. It is well known that the $B_{\text{ISV}}M1\uparrow$ and the B(GT) differ in their quenching by about 25%. Systematics show[37] that this difference is nearly uniform over many nuclear levels in this region. Thus we obtained the "corrected" λ_{NX} by multiplying the "uncorrected" one by 0.75. The λ_{NX} so obtained are compared in Table III with those derived from the

TABLE III. Comparison of NUEX strengths in ^{11}B obtained from radiative and (p,n) reaction data.

State	$B(M1)\uparrow$ (Expt)	$B(M1)\uparrow$ (Th)	$B_{\text{ISV}}(M1)\uparrow$ (Th)	$B_{\text{ISV}}(M1)\uparrow$ ("Expt")	λ_{NX} (Rad.)	λ_{NX} (p,n)
2.12	0.575(45)	0.868	0.950	0.63(5)	0.142(10)	0.159(16)
4.45	0.900(90)	0.785	0.896	1.03(10)	0.231(23)	
5.02	1.25(5)	1.124	0.915	1.02(4)	0.231(10)	
Doublet					0.46(3)	0.38(4)

TABLE IV. Solar-neutrino yields (standard model) for ^{11}B.

NUEX ($^{11}B \rightarrow ^{11}B^*$)			CC ($^{11}B \rightarrow ^{11}C, ^{11}C^*$)		
E (MeV)	λ_{NX}[a]	Y_{NX}[b]	E (MeV)	λ_{CC}[a]	Y_{CC}[b,c]
			0	1.55	772
2.12	0.15	60	2.00	0.6	161
4.45	0.21	36	4.32	0.84	83
5.02	0.21	28	4.81	0.84	63
Total NUEX (to 4.45 + 5.02)		64	Total CC		1079

[a]Average of radiative and (p,n) data.
[b]Yield/100 metric tons of boron/year.
[c]Yield for total event energy $E > 4$ MeV.

B(GT) values from (p,n) reaction data.

The experimental shapes of the (p,n) spectra[7] for the 5-MeV doublet at two different resolving powers appear symmetrical at two different resolving powers, supporting the equality of λ_{NX} predicted in Table III. The agreement of the two sets of λ_{NX} values and thus the mutual confirmation of the two widely different methods is satisfactory.

Using the above data, the calculated solar-ν event rates for the NUEX and CC transitions in the ^{11}B-^{11}C system for the SSM ^{8}B flux of $\phi = 6\times10^6$/cm^{2}sec are listed in Table IV.

[1]S. Weinberg, in *Proceedings of the XXIII International Conference on High Energy Physics,* Berkeley, California, 1986, edited by S. Loken (World Scientific, Singapore, 1987).

[2]J. K. Rowley, B. T. Cleveland, and R. Davis, Jr., in *Solar Neutrinos and Neutrino Astronomy* (AIP Conf. Proc. No. 126) (AIP, New York, 1984), pp. 1–21.

[3]S. P. Mikheyev and A. Y. Smirnov, Nuovo Cimento C **9**, 17 (1986).

[4]L. Wolfenstein, Phys. Rev. D **17**, 2369 (1978); **20**, 2634 (1979).

[5]R. S. Raghavan, S. Pakvasa, and B. A. Brown, Phys. Rev. Lett. **57**, 1801 (1986).

[6]H. C. Lee, Nucl. Phys. **A294**, 473 (1978).

[7]T. Taddeucci, private communication.

[8]The value for λ_{NX} (4.38 MeV) in Ref. 5 should be 0.91 instead of the incorrectly transcribed value of 1.5.

[9]See, e.g., J. N. Bahcall, Phys. Rev. **136**, B1164 (1964).

[10]J. B. Birks, *Theory and Practice of Liquid Scintillation Counting* (Pergamon, New York, 1964).

[11]K. Hirata *et al.*, Phys. Rev. Lett. **58**, 1490 (1987).

[12]P. Lagage, Nature (London) **316**, 420 (1985).

[13]L. M. Krauss, S. L. Glashow, and D. N. Schramm, Nature (London) **310**, 191 (1984).

[14]For a review, see R. T. Rood, in Proceedings of the Conference on Status and Future of Solar Neutrino Research, Brookhaven National Laboratory, 1978 [Brookhaven National Laboratory Report No. BNL-50879 (unpublished)], pp. 175–206.

[15]J. N. Bahcall *et al.*, Astrophys. J. **292**, L79 (1985).

[16]J. N. Bahcall, in *Weak and Electromagnetic Interactions in Nuclei,* edited by H. V. Klapdor (Springer, Berlin, 1986), pp. 705–709.

[17]J. Faulkner and R. L. Gililand, Astrophys. J. **299**, 994 (1985).

[18]J. Faulkner *et al.*, Nature (London) **321**, 226 (1986); R. Dappen *et al.*, *ibid.*, **321**, 228 (1986).

[19]Z. Maki, M. Nagakawa, and S. Sakata, Prog. Theor. Phys. (Kyoto) **28**, 870 (1962).

[20]B. Pontecorvo, Zh. Eksp. Teor. Fiz. **53**, 1717 (1967) [Sov. Phys. JETP **26**, 984 (1968)].

[21]L. B. Okun *et al.*, Yad. Fiz. **44**, 677 (1986) [Sov. J. Nucl. Phys. **44**, 440 (1986)].

[22]V. Barger, K. Whisnant, and R. J. N. Phillips, Phys. Rev. D **24**, 538 (1981).

[23]H. A. Bethe, Phys. Rev. Lett. **56**, 1305 (1986).

[24]S. P. Rosen and I. Gelb, Phys. Rev. D **34**, 969 (1986).

[25]S. Parke, Phys. Rev. Lett. **57**, 2322 (1986).

[26]A. J. Baltz and J. Weneser, Phys. Rev. D **35**, 528 (1987); A. J. Baltz and J. Weneser, in Proceedings of the Brookhaven National Laboratory Workshop, Brookhaven National Laboratory, 1987 [Brookhaven National Laboratory Report No. BNL-5208 (unpublished)], p. 121.

[27]J. Bouchez *et al.*, Z. Phys. C **32**, 499 (1986).

[28]M. Cribier *et al.*, Phys. Lett. B **182**, 89 (1986).

[29]S. M. Bilenky and B. Pontecorvo, Phys. Rep. **41**, 225 (1978); Nuovo Cimento **17**, 569 (1976).

[30]P. Langacker *et al.*, Nucl. Phys. **B282**, 589 (1986).

[31]W. Hampel, in *Solar Neutrinos and Neutrino Astronomy* (Ref. 2).

[32]A. Cisneros, Astrophys. Space Sci. **10**, 87 (1971).

[33]H. Chen, Phys. Rev. Lett. **55**, 1534 (1985).

[34]C. Rubbia *et al.*, Istituto Nazionale di Fisica Nucleare Report No. INFN/AE-85/7, 1985 (unpublished).

[35]S. Raman *et al.*, Nucl. Data Table **21**, 567 (1978).

[36]F. Ajzenberg-Selove, Nucl. Phys. **A336**, 1 (1980).

[37]B. A. Brown and B. H. Wildenthal, Phys. Rev. C **28**, 2397 (1986).

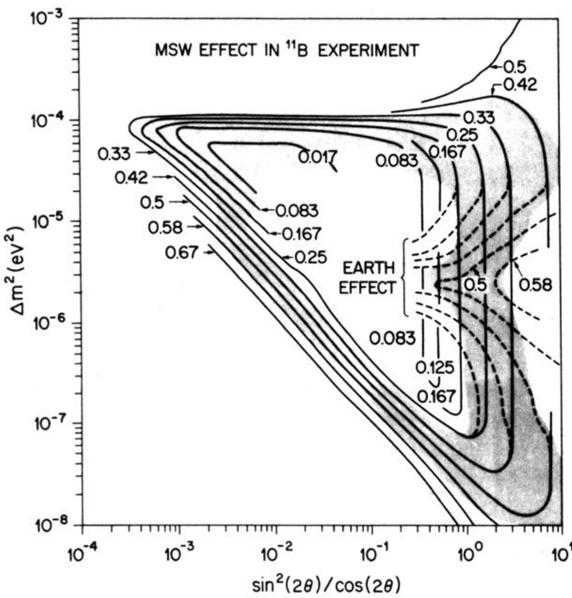

FIG. 3. CC survival fraction S for ν parameters Δm^2 and $(\sin^2 2\theta/\cos 2\theta)$ relevant to the MSW effect. The solid lines are iso-S contours. The shaded region is the space compatible with the Homestake experiment according to 5.9 SNU SSM(A) (reproduced with kind permission from A. J. Baltz).